DEPTH AND DIAMETER OF TRANSIENT CRATERS. S. Yamamoto[1], N. Okabe[1], K. Wada[2], and T. Matsui[1], [1]Graduate School of Frontier Sciences, University of Tokyo, Tokyo 113-0033, Japan (yamachan@gfd-dennou.org). [2]Department of Earth and Planetary Sciences, University of Tokyo, Tokyo 113-0033, Japan

Introduction: Transient crater in gravity regime collapses even during excavation stage owing to gravity, and the crater shape (diameter and depth) may change. In the previous experiments [e.g.,1], crater shapes after the collapse have been assumed to be the same as those of transient craters, because the degree of the collapse has been considered to be negligible in laboratory scales. However, even in laboratory scales, the degree of the collapse may depend on target material properties (e.g., cohesion among grains). Therefore, we tried to observe formation process of transient craters directly.

Experiments: Figure 1 shows the schematic diagram of experimental apparatus. Polycarbonate projectiles with mass of 0.49 g and diameter of 10 mm were accelerated by a single-stage gas gun. Impact velocities ranged from 44 to 321 m/s. The impact angles to the target surface were vertical. We prepared soda-lime glass spheres with mean sizes (s) of 40, 80, and 220μm as the target material. The glass spheres were placed in a stainless basin with depth of 9.0 cm in the vacuum chamber with the ambient pressure < 90Pa.

Results:(1) Transient crater diameter. Formation and collapse processes of transient craters were observed by a camcorder set at the port with angle of 45° on the experimental chamber (Fig.1). We can take images at a time interval of 1/30s by the camcorder. Figure 2b shows an example of the image of crater taken by the camcorder for the case of mean grain size of 80μm and impact velocity of 309m/s. The light source was set along the target surface from the direction perpendicular to Fig.1. From the analysis of the image (Fig. 2b), we can determine a rim diameter at each time step (the arrows in Fig.2b indicate the crater rim).

Figure 2a shows the growth of a rim diameter with time. As shown in this figure, the transient crater formed within 0.2s from the instance of contact. The rim diameter of the transient crater (transient rim diameter) was about 120 mm in this case. The crater started collapsing at about 0.7s, and then the rim diameter increased from 120 mm to 131 mm. The collapse halted at 2s and the final crater was formed.

By using this method, we can measure transient rim diameter D_t and final rim diameters D_f for a variety of impact velocity and grain sizes. The average ratios of D_f /D_t were 1.04, 1.05, and 1.06 for s=40, 80, and 220μm, respectively.

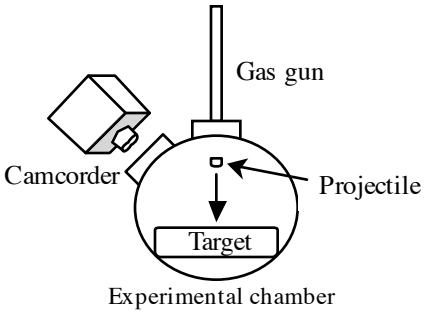

Figure 1: Schematic diagram of the experimental apparatus (side view).

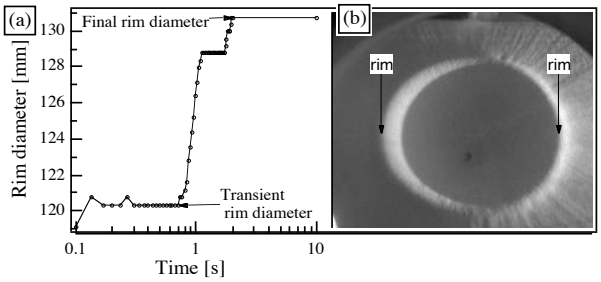

Figure 2: (a) Growth of a rim diameter for target spheres with mean size of 80μm and impact velocity of 309 m/s. (b) The image of the crater at 0.4 s from the impact for the same experiment of (a).

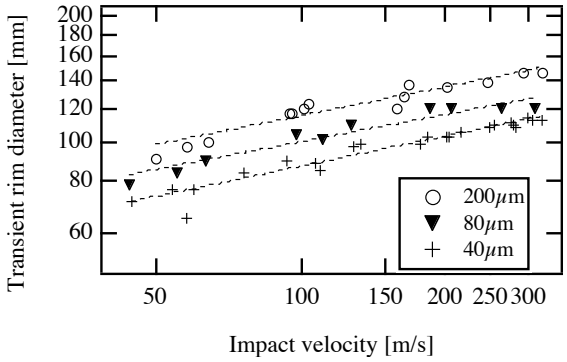

Figure 3: (a) A rim diameter of a transient crater is plotted against impact velocity. Dashed line indicates the best–fit curve.

In Figure 3, the transient rim diameters D_t are plotted against the impact velocities v. It is clear from this figure that D_t increases with an increase in v. Figure 3 also shows clearly that D_t increases with an increase in grain size s. Assuming a power-law relation between D_t and v, the slopes (dashed line in Fig.3) for s=40, 80, and 220μm were estimated to be 0.245, 0.229, and 0.245, respectively. Although the power-law exponents for three targets were similar, the present results show that the

transient crater radii vary with grain sizes.

(2) Transient crater depth. Next, we measured the depths d of transient craters from the original target surface. It is difficult to measure the depths from the images taken by the camcorder. Thus, in the present experiments, a penetration depth of a projectile was assumed to be the transient crater depth. By using a way of 'quarter-space' technique as will be described in discussion, we can demonstrate that the difference between H and the penetration depths of projectiles was less than 10%. After shots, the penetration depths from the original target surface were measured directly. In Figure 4, the transient crater depth d is plotted against the impact velocity v. We can see that d increases with an increase in v, which are similar to that of the transient rim diameters (Fig.3). However, the differences due to the grain size s are smaller compared with those of Fig.3. It has been shown that the penetration depths of projectiles to porous targets mainly depend on the target bulk densities [2]. The bulk densities of the targets were measured to be 1.49, 1.53, and 1.56 g/cm^3 for s=40, 80, and 220μm, respectively. In the present experiment, the difference in bulk densities may be too small to cause the significant differences in penetration depths of projectiles.

Discussion: We conducted the additional experiments by using a way of 'quarter-space' technique [e.g.,3]. The glass spheres with s=80μm were set in a sample box with a transparent window. The projectile impacted the target surface adjacent to the transparent window, so that we can observe the excavation process directly by using the camcorder. Figure 5a shows an example of the image of an excavation flow at 1/30s from the impact (v=154m/s). We can see the cavity due to the excavation flow. The x-axis corresponds to the target surface. The projectile impacted the target surface along y-axis. In Figure 5b, contours of the cavities due to the excavation flow below the x-axis were traced from three images at 1/30, 2/30, and 3/30s from the impact (Figs.5a and 5b are the same experiment). The growth of the excavation flow halted at 2/30s, because the depths of the cavities (measured from the x-axis) at 2/30 and 3/30s are the same. On the contrary, the radial expansion of the cavity along the x-axis continued after the growth of the excavation flow had halted. It is noted that the shape of cross section of the cavity at the first image (1/30s) is nearly hemispheric, while the ratio of rim diameter over depth as shown in the third image (3/30s) became larger. The ratios of the rim diameter to the cavity depth at 1/30s and 3/30s were measured to be 2.3 and 4.2, respectively.

This observation might be interpreted as follows: During the early stage of the excavation processes, the dynamical pressure of the excavation flow is high enough to dominate over effects of material properties. Thus, the shape of the cavity of the excavation flow can become nearly hemispheric. On the other hand, the dynamical pressure of the flow in the radial expansion of the cavity in the final stage (from 2/30 to 3/30s in Fig.5b) is low, so that the radial expansion process would be perturbed by material properties such as cohesion (or friction) among grains. The cohesion (or friction) could depend on grain sizes. This might be the reason why the transient rim diameters showed the grain size dependence.

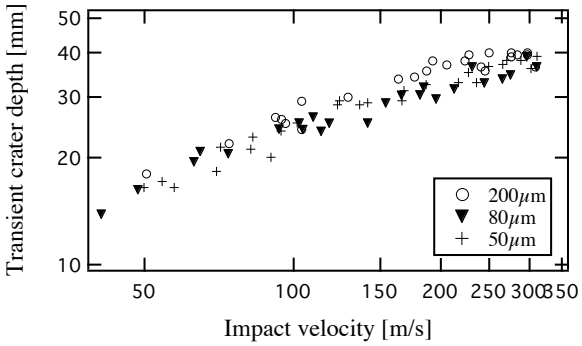

Figure 4: A depth of a transient crater from the original target surface is plotted against impact velocity.

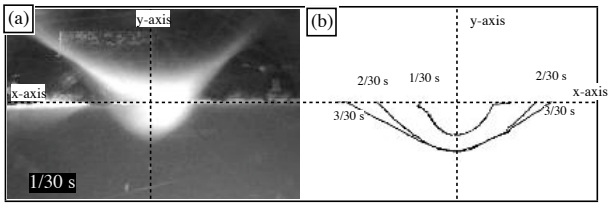

Figure 5: (a) The image of excavation flow at 1/30s from the impact. The x-axis corresponds to the original target surface. The projectile impacts the target along y-axis. (b) Contours of the cavities of the excavation flow below x-axis. The number at each curve is the time from the impact.

References: [1] Schmidt R.M., 1980, *Proc. LPSC* 11th, 2099-2128. [2] Kadono T., 1999, *Planetary Space Science*, 47, 305-318. [3] Schmidt R.M., and Piekutowski, A.J., 1983, *Proc. LPSC* 14th, 668-669.